Analysis of the atmosphere behaviour in the proximities of an orographic obstacle

E. Hernández, J. Díaz, L. C. Cana, A. García

Nonlinear Processes in Geophysics (1995) 2: 30 - 48

Nonlinear Processes in Geophysics

Analysis of the atmosphere behaviour in the proximities of an orographic obstacle

E. Hernández[1], J. Díaz[2], L. C. Cana[1] and A. García[1]

[1] Departamento de Astrofísica y Ciencias de la Atmósfera, Facultad de Ciencias Físicas, Universidad Complutense, 28040 Madrid, Spain
[2] C.U.S.P. Medio Ambiente, General Oraá 39, 28006 Madrid, Spain

Received 15 April 1994 - Accepted 28 November 1994 - Communicated by A. Provenzale

Abstract. The atmospheric behaviour near an orographic obstacle has been thoroughly studied in the last decades. The first papers in this field were mainly theoretical, being more recent the laboratory experiments which represented that behaviour in ideal conditions. The numerical simulations have been addressed lately thanks to the development of computers. But the study of Meteorology in complex terrain has lacked experiments in the atmosphere to understand the real influence the relief has on it.

In this paper the problem has been considered from the last perspective, and so, seasons of measure of the atmospheric variables within the boundary layer have been organised with the goal of checking existing theories and bringing right conclusions from real experiment in the atmosphere.

Controverted aspects of linear and nonlinear theories, as the location of the critical points upwind and downwind of an orographic obstacle, will be analysed. The results obtained show a large adequacy between the forecasted behaviour and the experimentally detected.

1 Introduction

Progress in the knowledge of Mountain Meteorology has shown the influence orography has on those meteorological parameters which characterise the atmosphere from both the thermal and dynamical points of view. These perturbations show themselves through different phenomena peculiar to complex orography, the most evident of which may be the formation of characteristic clouds such as fog, lines of cumuli or cumuli-strata, nacred clouds, etc.

Even if the atmospheric conditions don't allow the formation of these clouds, mountainous obstacles clearly affect the behaviour of wind in their proximities.

Computer simulations such as those realised by Smolarkiewicz et al. (1988), Smolarkiewicz and Rotunno (1989) and Miranda and James (1992), as well as the laboratory studies by Hunt and Snyder (1980) and Castro (1987) have shown the evidence of the formation of lee waves and lee vortices.

Rayleigh (1883) and Kelvin (1886) started the theoretical study of the evolution of a fluid downstream of an obstacle. Ever since there has been lot of research about mountain waves.

Nowadays there are two mainstream theories: the potential flow theory, established by Drazin (1961), and Smith's linear theory (1980). These theories which may be applied depending on the atmospheric conditions and on the size of the obstacle, are, according to Smith himself, "different and unconnected, although qualitatively they complete each other". Later, Smith (1993) modifies the linear theory introducing nonlinear aspects in order to explain stagnation points and bifurcation in 3-D mountain airflow. The most surprising aspect of this theory is probably the suppression of the stagnation point upwind of the mountain which favours stagnation downwind of the mountain. These aspects will be analysed in the discussion of the wind speed results.

Regarding how many theoretical studies and computer simulations have been carried out in these last years, we should remark that very few of these works are based on real atmospheric data, the most interesting of these being those by Blanchard and Howard (1986), Feber and Mass (1990 a, b).

Some of the results about the behaviour of the atmosphere obtained as a consequence of the field experiments held in the years 1991 and 1992 (Díaz, J., 1993) will be shown. Their main points are:

1. Experimentally registering the behaviour and temporal evolution of several meteorological variables and parameters at both sides of a mountain range under a flow normal to it.

2. Empirically detect the existence of some dynamic structures at the downwind slope of a mountain and analyze their temporal evolution.

2 Theoretical considerations

To achieve a quantitative explanation of the apparition of lee waves we will follow Holmboe and Klieforth (1957). We will make the following basical considerations:

1. Linearization of the equations of motion. This hypothesis limits the type of orography which the equations can be applied to, since the mountain height must be small in relation with its width, which happens to be quite usual in nature.

2. The friction, the condensation and the heat of conduction and radiation are neglected. This way anisotropic effects are excluded. Though this hypothesis

excludes condensation, which is closely related to lee waves, it proves not to be very limiting in our experimental environment.

3. Earth's rotation is neglected. This fact is perfectly assumable because of the small horizontal scale of the phenomenon studied.

4. Stationary flow. The dependence on time in the basic equations will be removed.

5. Bidimensional problem. The study will be limited to an isolated obstacle perpendicular to the direction of basic flow, which is supposed to go towards the positive extreme of the X axis.

The variables are:

Speed: $\bar{u}(z) + u(x,z),\ w(x,z)$

Pressure: $\bar{p}(z) + p(x,z)$

Density: $\bar{\rho}(z) + \rho(x,z)$

Temperature: $\bar{T}(z) + T(x,z)$

Where the magnitudes with a bar refer to undisturbed values and the other quantities refer to deviation from the undisturbed values. With these hypotheses, the basic equations can be written as follows

Momentum:

$$(\bar{u} + u)\frac{\partial u}{\partial x} + w\frac{\partial \left(\bar{u} + u\right)}{\partial z} = -\frac{1}{\bar{\rho} + \rho}\frac{\partial p}{\partial x} \quad (1)$$

$$(\bar{u} + u)\frac{\partial w}{\partial x} + w\frac{\partial w}{\partial z} = -\frac{1}{\bar{\rho} + \rho}\frac{\partial \left(\bar{p} + p\right)}{\partial z} - g \quad (2)$$

Matter:

$$(\bar{u} + u)\frac{\partial \rho}{\partial x} + w\frac{\partial \left(\bar{\rho} + \rho\right)}{\partial z} = -\left(\bar{\rho} + \rho\right)\left(\frac{\partial u}{\partial x} + \frac{\partial w}{\partial z}\right) \quad (3)$$

Energy:

The equation of energy for an adiabatic process in the real state can be written this way:

$$c_p + \frac{d\,Ln\,T}{d\,t} = R\frac{d\,Ln\,p}{d\,t} \quad (4)$$

The previous equations are completed with the equation of gases

$$\frac{\bar{p} + p}{\bar{\rho} + \rho} = R\left(\bar{T} + T\right) \quad (5)$$

in which R is the constant of gases $R = c_p - c_v$, so the equation of continuity can be expressed as follows:

$$\overline{M} + w_{xx} + w_{zz} - \left(\bar{s} + \frac{\overline{M'}}{\overline{M}}\right)w_z + \left[\left(\bar{\rho} + \frac{\overline{M'}}{\overline{M}}\right)\frac{g}{\bar{u}^2} + \left(\bar{s} + \frac{\overline{M'}}{\overline{M}}\right)\frac{\bar{u}'}{\bar{u}} - \frac{\bar{u}''}{\bar{u}}\right]w = 0 \quad (6)$$

Where the suffixes denote partial derivatives and the apostrophe derivatives with respect to z of the undisturbed magnitudes. Therefore, it is a differential equation in second order partial derivatives for the vertical velocity w(x,z).

In Eq.(6). new variables have been introduced so that a more simplified expression can be obtained:

$$\overline{M} = 1 - \frac{\bar{u}^2}{\bar{c}^2} \tag{7}$$

$$\bar{s} = \frac{d \ln \bar{\rho}}{dz} \tag{8}$$

$$\bar{\sigma} = \bar{s} - \frac{g}{\bar{c}^2} \tag{9}$$

Expression (7) stands for the deviation of Mach's number from unit for undisturbed flow. In the atmosphere $\bar{u}^2 << \bar{c}^2$ so $\overline{M} \cong 1$.

$\bar{s}$ in Eq. (8) stands for the vertical gradient of density which as $\frac{\bar{s}}{2}$, was called factor of heterogeneity by Queney (1947).

$\bar{\sigma}$ stands for the degree of stability of the atmosphere. To simplify Eq (6) we may call:

$$\bar{S} = \bar{s} + \frac{\overline{M'}}{\overline{M}} \tag{10}$$

$$\bar{\beta} = \bar{\sigma} + \frac{\overline{M'}}{\overline{M}} \tag{11}$$

Doing the adequate changes and eliminating terms in Eq. (6) we finally get:

$$\overline{M}\, w_{1xx} + w_{1zz} + F(z)\, w_1 = 0 \tag{12}$$

This equation represents the anomalies of w at each point of the z-x plane which are proportional to w itself. The factor of proportionality is given by F(z), whose value is:

$$F(z) = \frac{\overline{\beta}\, g}{\bar{u}^2} + \frac{\overline{S u'}}{\bar{u}} - \frac{1}{4}\bar{S}^2 + \frac{1}{2}\bar{S}' - \frac{\bar{u}''}{\bar{u}} \tag{13}$$

This function of z has five terms that take account of the contributions of the dynamical and thermal phenomena to the anomalies of the vertical velocities. The contributions are of very different orders of magnitude, as it is shown in the following analysis.

2.1 Analysis of equation (13)

If we consider the definition of each term of this equation and accepting that $\bar{u}^2 << \bar{c}^2$, we can calculate, from the data provided by the aerological soundings with a captive balloon, the addends appearing in Eq. (13) and analyse their contribution to F(z). Table 1 shows some examples of these contributions provided by the aerological soundings realised in these experimental seasons.

HOUR GMT	06:00	08:00	10:00	12:00	16:00
$\beta g/u^2$ (10^{-6} m^{-2})	25.6	8.1	2.5	-0.9	-1.8
$\delta u'/u$ (10^{-6} m^{-2})	2.0	-3.1	-1.8	13.1	1.6
$S^2/4$ (10^{-6} m^{-2})	3.8	5.3	5.8	5.6	5.8
$S'/2$ (10^{-6} m^{-2})	-7.3	2.8	-2.9	-0.1	8.7
u''/u (10^{-7} m^{-2})	-14.8	-4.6	-2.5	-6.7	-1.3
$\lvert u u''/g\beta \rvert$	0.06	0.06	0.10	0.74	0.07

Table 1. Analysis of scale of Eq. (15). Piedralaves 07/08/92

In this table we can observe that the order of magnitude is about 10^{-6} for $\frac{\overline{\beta}\,g}{\bar{u}^2}$; 10^{-8} for $\frac{\overline{S\,u'}}{\bar{u}}$; 10^{-9} for $\frac{1}{4}\,\bar{S}^2$ and $\frac{1}{2}\,\bar{S}'$; and 10^{-7} for $\frac{\bar{u}''}{\bar{u}}$ so, in a first approach, we can neglect the contribution to F(z) by all these terms except for Scorer's parameter and the wind shear and write the equation as:

$$F(z) = \frac{\overline{\beta}\,g}{\bar{u}^2} - \frac{\bar{u}''}{\bar{u}} \qquad (14)$$

Scorer (1949) made a study about the contribution of the u" term to F(z) in which, from a approximated profile of the wind changes with height, he concluded that in the first 900 m over the surface the values of $\frac{\bar{u}''\,\bar{u}}{\overline{\beta}\,g}$ fluctuate between 0.36 and 0.49 and the wind shear can't be neglected. If we take into account all the soundings we have done and make an analysis of scale we observe a contribution to F(z) by this term minor than 10% in 85% of the soundings. Eliminating those soundings corresponding to an unstable atmosphere, which are not interesting for the formation of mountain waves, the contribution of this term will be minor than 10% of the total, and so, it can be neglected. We can write:

$$F(z) = \frac{\overline{\beta}\,g}{\bar{u}^2} = \frac{1}{\bar{u}^2}\,\frac{g}{\theta}\,\frac{\partial\theta}{\partial z} = l^2 \qquad (15)$$

which represents Scorer's parameter (l^2). In this expression $\bar{u}^2$ is the average wind speed in the considered layer and $\frac{\partial\theta}{\partial z}$ is the vertical gradient of potential temperature. This parameter physically represents a wave number and we can associate a wavelength to it. In each layer we can calculate it with a positive value.

3. Experimental process.

As we have seen, the fundamental objective of this work is to experimentally calculate the behaviour of the atmosphere at both sides of a mountainous range. For that reason we'll have to calculate different meteorological parameters to characterise it both thermal and dynamically. Also, we will analyse the different atmospherical patterns shown by the referenced numerical simulations and laboratory experiments. Therefore, the measure seasons should allow us to know, at both sides of the mountain, the desired atmospherical variables. This study will be centred on the first one thousand meters over the surface, a very important region but seldom analysed by researchers.

The kind of work to be done makes very important to select a good experimental location. It is important to localise a mountainous range long enough to allow a bidimensional treatment. Both sides of the range the terrain must be as plain as possible to avoid the influence of obstacles on the magnitudes which are to be measured.

The linearization of these equations of movement

requires the height of the mountain to be small in relation with its width.

The Sistema Central has been selected as the right place for the experiment for these reasons and, besides, its geographical proximity to Madrid. There were some previous data from this area since the application of a diagnostic model of the wind field in complex orography (Hernández et al. 1992,a, b, 1993) in a previous stage.

The experimental seasons took place in the Gredos area of the Sistema Central mountain range. The locations selected were Burgohondo and the Tietar Air Field, near Piedralaves. Burgohondo is at the northern slope of the mountain with an altitude of 880 m, it's a plain and open area a few kilometres south of the Sierra de la Paramera range. The Tiétar Air Field is in a wide valley south of Sierra de Gredos, its altitude being 427 m.

Both places are 20 km away. The average altitude of the Sistema Central in the proximities of the experimental location is 1600 m, and the highest point in the line linking both places is 1827 m. In this section, the mountainous range can be taken as the axis of symmetry of the line linking both experimental locations.

In this experiment we intend to analyse the behaviour of the atmosphere at both sides of a mountain range under different meteorological conditions, which will be defined by Froude's number Fr = U/N h, where U is the average wind speed; N is the Brunt-Väisällä frequency and h the height of the obstacle. In the numerical simulations by

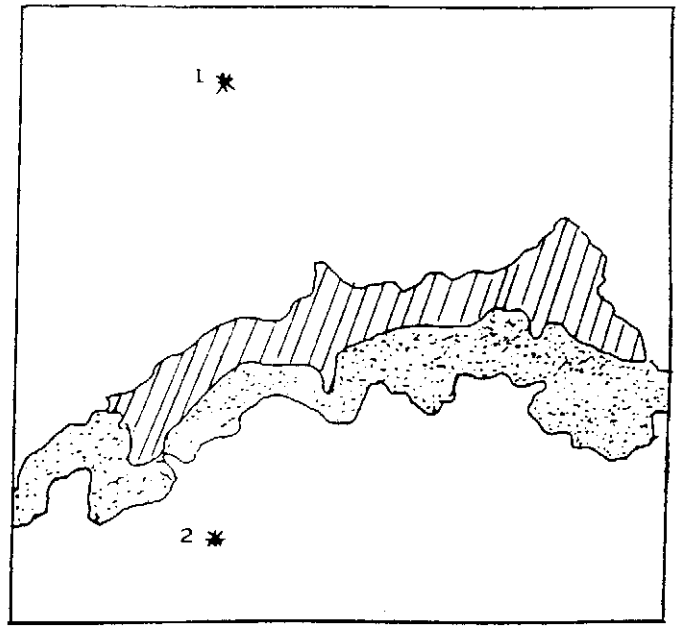

Figure 1. Location of experimental sites

1. Burgohondo 2. Piedralaves

Smolarkiewicz et al. (1988) and Miranda and James (1992) this parameter ranged from 0 to 10. The one opportunity to guarantee this range of oscillation in the atmosphere is through N. For this reason the season of choice had to be summer: there is a very stable atmosphere in the early morning with Fr values near zero, while almost neutral stratifications and larger values of Fr may appear later.

In order to register this oscillation, we made our aerological soundings at 06:00, 08:00, 10:00, 12:00, 16:00h G.M.T. every day of the two experimental seasons: The first one from July 7 to 10 1992, and the

second one from September 8 to 11, 1992. The variables measured are: pressure, wind speed, wind direction, dry bulb temperature and wet bulb temperature. From these magnitudes, and through the usual conversions, we have determined the height, relative humidity, potential temperature, etc.

The data have been collected through simultaneous captive aerological soundings at both sides of the mountain. The sensors had been previously compared through statical and dynamical tests, so we can say that the different values of certain magnitudes are due to physical and not to instrumental reasons.

4 Wind field analysis.

4.1 Wind direction.

As we have seen, there are many meteorological patterns occurring at the downwind slope of a mountain, which are different from those at the upwind slope. It seems clear that a first step is to analyse the wind direction for each day for which there is an aerological sounding. There are only two days in which the wind followed quite a constant direction. The first one is July 8, 1992. That day the wind direction above surface ranged between 320 and 40 degrees at Burgohondo, while at Piedralaves it ranged from 90 to 290 degrees. Taking into consideration the orientation of the mountain range, we can conclude that Burgohondo is placed upwind and Piedralaves is placed downwind of the range.

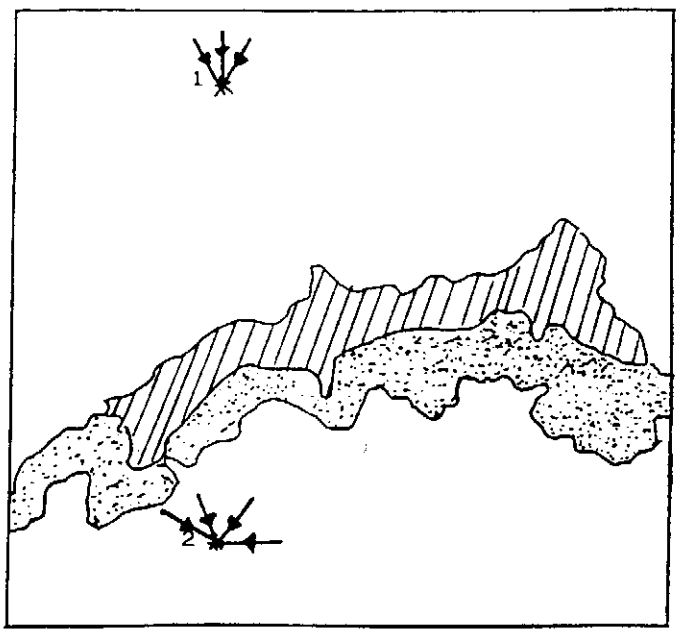

Figure 2. Wind direction on 07/08/92.

The second day is September 10, 1992. At Burgohondo the direction ranged from 200 to 210 degrees, and at Piedralaves the wind direction ranged from 180 to 210 degrees. So, Burgohondo is placed downwind and Piedralaves is placed upwind of the range.

4.2 Wind speed.

Once the experimental locations have been oriented in relation with the wind direction, we will analyse the

behaviour of the wind speed at both sides of the mountain. The presence and evolution of possible stagnation points and the possible linear models to evaluate the atmospheric conditions under which it is possible to extrapolate the values of the speed registered at the other slope will be studied.

A stagnation point can be defined as a place where the wind speed decreases considerably with respect to its environment. Sheppard (1956) used a kinetic energy balance and realised that for flows in which h > U/N (being h the mountain height, U the incident wind and N the Brunt-Väisällä frequency), the wind can't flow over the obstacle without stagnation points appearing, not regarding the mountain shape. That problem was studied by Smith (1988) using the linear theory for an asymmetric mountain and a shearless flow. Later on, Smith (1989) analyzed the case with shear and concluded that there are two points where the wind speed decreases, one at the upwind (B) slope and the other in the downwind side (A), at a higher level. There is another critical point (C) at the downwind slope, lower than (A), where the wind speed is maximum.

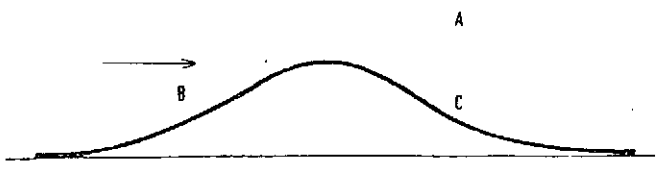

Figure 3. Critical points according to Smith.

Hunt and Snyder (1980) and Smolarkiewicz and Rotunno (1990) realised that the point (B) should be in relation with the flow separation needed to make the flow surround the obstacle instead of passing over it. The apparition of stagnation points may also be connected with the production of vorticity at the downwind slope, which can generate vortices according to Smolarkiewicz and Rotunno (1989) and Crook et al. (1990).

Smith (1993) worked on this problem and elaborated a theory where the nonlinearity was taken into account. Some differences between these two theories appear in the critical value under which Froude's number produces a stagnation point: The linear theory places it at about 0.7 and the nonlinear theory puts it at 0.9. Perhaps the most surprising point is that the nonlinear theory eliminates the stagnation point B at the upwind slope.

HOUR	Fr
06:00	0.11
08:00	0.25
10:00	0.38
12:00	----
16:00	----

Table 2. Values Fr on 07/08/92

Table 2 shows the values of Froude's number (Fr) registered in each sounding realised on July 8, 1992. The "---" lines refer to a global instability of the atmosphere, where Fr cannot be computed.

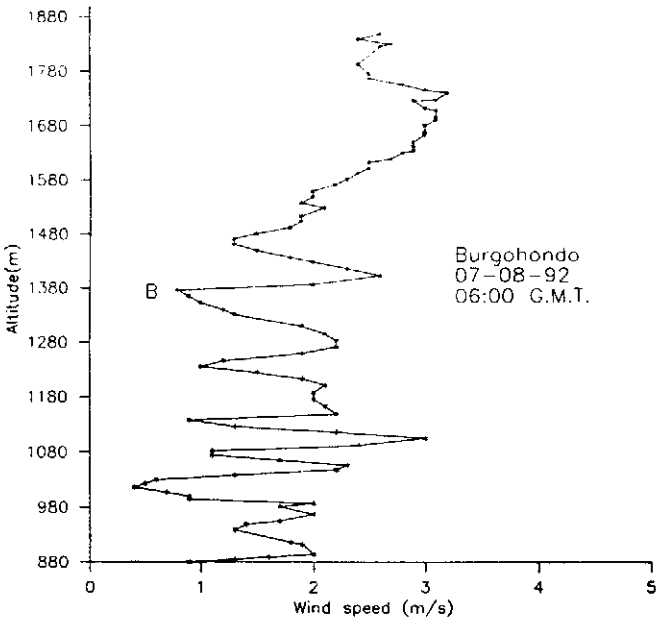

Figure 4. Wind speed -height. Burgohondo 07/08/92

06:00 G.M.T.

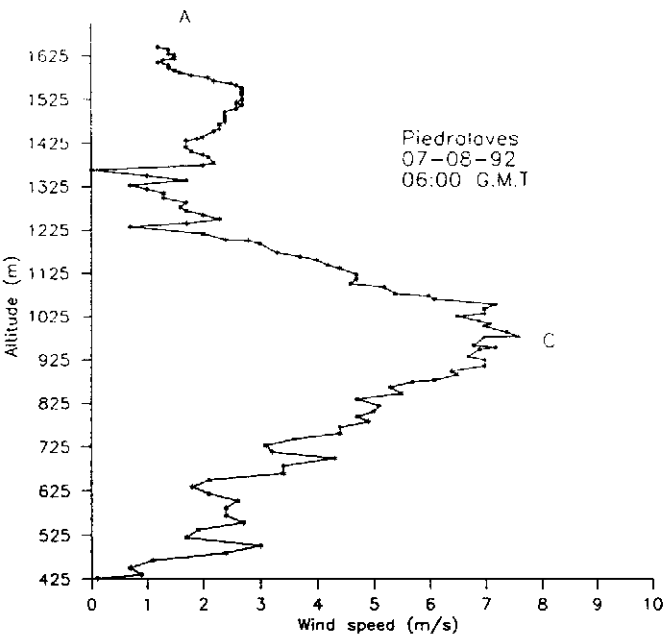

Figure 5. Wind speed -height. Piedralaves 07/08/92

06:00 G.M.T.

Figures 4 and 5 show the profiles of wind speed in relation with height for each sounding site on July 8 1992 at 06:00 G.M.T. If we analyse these graphics, we can observe that two points of minimum wind speed appear in Burgohondo, this time in the upwind slope, one close to the ground and the other (B) at 450 m above it. Let's remember that the mountain height, measured from this place, is 1000 m. It agrees with Smith's theoretical prediction, which situates this stagnation point near the middle of the mountain, and with Peltier and Clark's (1979) who situated that point at 3/4 $2\pi U/N$ above the ground, what means 500 m according to the 06:00 G.M.T data. From this point the wind speed increases.

Figure 5 shows a clear maximum of wind speed between 500 and 700 meters (C) at the downwind slope. As the mountain height from this side is 1400 m, this maximum is almost symmetric with the minimum at the upwind slope, which agrees with the theory. From the height of the maximum upwards the wind speed decreases, which agrees with the localisation of the downwind stagnation point, above the sounding top according to the simulations.

Our results partially corroborate the effects predicted by Smith's nonlinear theory (1993). The stagnation point upwind of the orographic obstacle (B) hasn't disappeared, but a new stagnation point (A) downwind of the mountain has appeared. As it is placed over the top of the sounding, no conclusions about its intensity can be drawn.

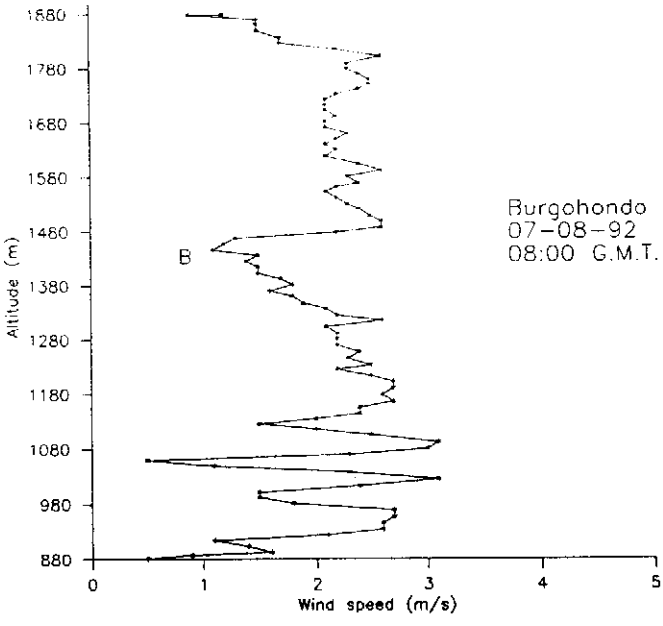

Figure 6. Wind speed -height. Burgohondo 07/08/92

08:00 G.M.T.

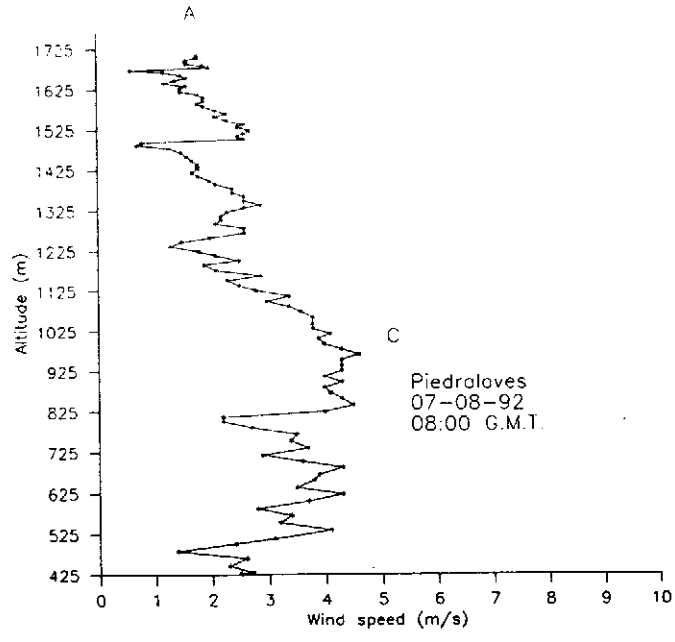

Figure 7. Wind speed -height. Piedralaves 07/08/92

08:00 G.M.T.

Figures 6 and 7 show the wind profiles corresponding to 08:00 G.M.T. at both observational sites. Their behaviour is similar to that at 06:00 h but with two important differences. The first one is their smoothing, i. e., at the upwind stagnation point the speed is higher and at the downwind maximum it is lower than at 6:00 h. Having in mind that Fr and, therefore, the ability of the flow to pass over the obstacle has increased, these changes should have been expected. Also, the upwind stagnation point has gone up the slope in the way it should have done, according to Peltier and Clark (1979), since the stability of stratification has decreased. By the way, the trend of the wind speed to decrease with a growing height increases when the top of the Piedralaves soundings rises, so reinforcing the hypothesis of an stagnation point at the downwind slope above the top of the mountain.

The results corresponding to the 10:00 G.M.T. soundings for Burgohondo show that, as we could expect since the stability has decreased, point (B) has kept ascending along this slope. In later soundings this behaviour has not been registered, since the instability of the stratification allows the flow to pass over the obstacle without any difficulty. The method used has consisted in establishing linear models for the values of U registered simultaneously and at the same height at both places. The results are shown in Tables 3 to 6.

If we consider the correlation coefficients corresponding to those days when the wind direction is approximately

THICKNESSES	POINTS	CORRELATION COEFFICIENT	LEVEL
50 m	394	0.36	99 %
100 m	193	0.37	99 %
200 m	90	0.40	99 %
300 m	58	0.42	99 %

Table 3. Correlation coefficients of U. Whole season.

THICKNESSES	POINTS	CORRELATION COEFFICIENT	LEVEL
50 m	80	0.11	No 95 %
100 m	40	0.10	No 95 %
200 m	18	0.16	No 95 %
300 m	12	0.26	No 95 %

Table 4. Correlation coefficients of U. Flow normal to the mountain range.

07/08/92.

THICKNESSES	POINTS	CORRELATION COEFFICIENT	LEVEL
50 m	79	0.11	No 95 %
100 m	39	0.11	No 95 %
200 m	18	0.10	No 95 %
300 m	11	0.23	No 95 %

Table 5. Correlation coefficients of U. Flow normal to the mountain range.

09/10/92.

THICKNESSES	POINTS	CORRELATION COEFFICIENT	LEVEL
50 m	176	0.46	99 %
100 m	88	0.48	99 %
200 m	42	0.60	99 %
300 m	27	0.58	99 %

Table 6. Correlation coefficients of U. Flow not normal to the mountain range.

perpendicular to the mountain range all day long, we can observe that, independently of being upwind or downwind, there isn't a correlation at the 95% level for any one of the thicknesses considered. But if we eliminate the data corresponding to these days the correlation is at the 99% level for all the thicknesses, being that of 200 m the one which presents the greatest coefficient. According to this, we can consider that the data collected at a mountain slope in days of perpendicular flow are not representative of the wind speed for the same height at the other slope, and, therefore, will not be useful as input for models which require of its knowledge.

5 Stability parameters

We have already studied the influence of an orographic obstacle from an exclusively dynamical point of view. This way, we will analyse the meteorological which take into consideration thermal and dynamical variables. Among the first ones, we'll consider Brunt-Väisällä frequency and among the second ones Scorer's parameter.

5.1 Brunt-Väisällä frequency.

It represents the vibration of a particle being separated from its equilibrium position in a stably stratified atmosphere. At each level, its value depends on whether the atmosphere is saturated. If we consider the meteorological situation and the season in which the data

were registered we can write:

$$N^2 = \frac{g}{\theta}\frac{\partial \theta}{\partial z} \qquad (18)$$

Equation (18), expressed in finite differences, computes N^2 from the data of the soundings for atmospherical strata with a variable thickness. A process similar to that used for wind speed is followed for Brunt-Väisällä frequency in order to establish linear models from data at both sides of the mountain (Tables 7,8,9 and 10).

THICKNESSES	POINTS	CORRELATION COEFFICIENT	LEVEL
50 m	394	0.37	99 %
100 m	193	0.50	99 %
200 m	90	0.67	99 %
300 m	58	0.69	99 %

Table 7. Correlation coefficients of Brunt-Väisällä frequency.

Whole season.

THICKNESSES	POINTS	CORRELATION COEFFICIENT	LEVEL
50 m	80	0.44	99 %
100 m	40	0.52	99 %
200 m	18	0.84	99 %
300 m	12	0.89	99 %

Table 8. Correlation coefficients of Brunt-Väisällä frequency. Flow normal to the mountain range. 07/08/92.

THICKNESSES	POINTS	CORRELATION COEFFICIENT	LEVEL
50 m	79	0.53	99 %
100 m	39	0.59	99 %
200 m	18	0.71	99 %
300 m	11	0.70	99 %

Table 9. Correlation coefficients of Brunt-Väisällä frequency. Flow normal to the mountain range. 09/10/92.

THICKNESSES	POINTS	CORRELATION COEFFICIENT	LEVEL
50 m	176	0.19	No 95 %
100 m	88	0.25	98 %
200 m	42	0.33	95 %
300 m	27	0.39	95 %

Table 10. Correlation coefficients of Brunt-Väisällä frequency. Flow not normal to the mountain range.

These tables show that the coefficients of correlation are at the 95% level when only the days without a definite flow are considered (except for a thickness of 50 m, which is under the 95% level and for 100 m thickness, which is at the 98% level). If we consider the data registered in days with a flow normal to the mountain range separately, the coefficients are always at the 99% level, not regarding the thickness. This behaviour is opposite to that of the wind speed.

5.2 Scorer's parameter

Studying this parameter is very important in Mountain Meteorology because it includes the thermal and dynamical aspects of the atmosphere. Besides, as we have seen, it has an associated wavelength under stability of stratification.

Equation (17) in finite differences calculates l^2 for atmospheric strata of different thickness from the data we have. This way, we have elaborated Tables 11 to 14.

THICKNESSES	POINTS	CORRELATION COEFFICIENT	LEVEL
50 m	392	0.22	95 %
100 m	193	0.36	99 %
200 m	90	0.36	99 %
300 m	58	0.42	99 %

Table 11. Correlation coefficients of Scorer's parameter.

Whole season

THICKNESSES	POINTS	CORRELATION COEFFICIENT	LEVEL
50 m	80	0.45	99 %
100 m	40	0.64	99 %
200 m	18	0.95	99 %
300 m	12	0.94	99 %

Table 12. Correlation coefficients of Scorer's parameter.

Flow normal to the mountain range. 07/08/92.

THICKNESSES	POINTS	CORRELATION COEFFICIENT	LEVEL
50 m	79	0.67	99 %
100 m	39	0.76	99 %
200 m	18	0.89	99 %
300 m	11	0.88	99 %

Table 13. Correlation coefficients of Scorer's parameter.

Flow normal to the mountain range. 09/10/92.

THICKNESSES	POINTS	CORRELATION COEFFICIENT	LEVEL
50 m	175	0.10	No 95 %
100 m	88	0.15	No 95 %
200 m	42	0.15	No 95 %
300 m	27	0.32	No 95 %

Table 14. Correlation coefficients of Scorer's parameter.

Flow not normal to the mountain range.

Since Brunt-Väisällä frequency and wind speed are included in Scorer's parameter and both showed an opposite behaviour as to the correlation coefficients and the presence of a definite flow, we could expect l^2 to have a behaviour intermediate to theirs. However, tables from 11 to 14 show that its behaviour is similar to that of the wind direction. The 200 m stratum is more sensitive to a definite wind direction, with a coefficient of 0.15 for a variable flow and 0.95 when there is a definite direction. The fact of this behaviour being the same at the upwind and downwind slopes proves that our conclusions do not depend on the topographical characteristics of the

experimental sites, but on their position with respect to the mountain range and the wind.

6. Waves and vortices downwind of a mountainous obstacle

The study of dynamic structures appearing at the downwind slope of a mountainous obstacle has been developed in these last years. There are different theories about the origin of these phenomena. Brighton (1978), Hunt and Snyder (1980) and Rottman and Smith (1989) have related it with the flow separation caused by viscous phenomena. Laboratory experiments by Brighton (1978), Hunt et al. (1980) and Rottman et al. (1989) explained it by the flow separation due to viscous phenomena. Numerical simulation by Smolarkievicz et al. (1989a) and Miranda et al. (1992) suppressed the viscous interaction, while these phenomena appeared anyway. These authors attributed these effects to density distribution. Smith (1989b) and Crook et al (1990) explained these effects by the dissipative phenomena related with the breaking of the waves downwind of an obstacle.

The objective of this work is to detect the formation of vortices at the downwind slope of a mountain using actual atmospheric data. Two methods will be used to achieve this: spectral analysis and the analysis of the wind direction and of the wavelengths associated to Scorer's parameter.

6.1 Spectral analysis.

The series to be analysed are formed by the wind speed registered during the soundings made at the experimental sites. The U values are collected 10 m away, interpolated where necessary.

Figures 8 and 9 show some series where we can detect periodicity. The Fast Fourier Transform is applied here. In these figures the X-axis represents the inverse of the wavelength and the Y-axis represents the normalized variance of the spectrum. The null continuous and the 90 and 95% levels of confidence are also shown.

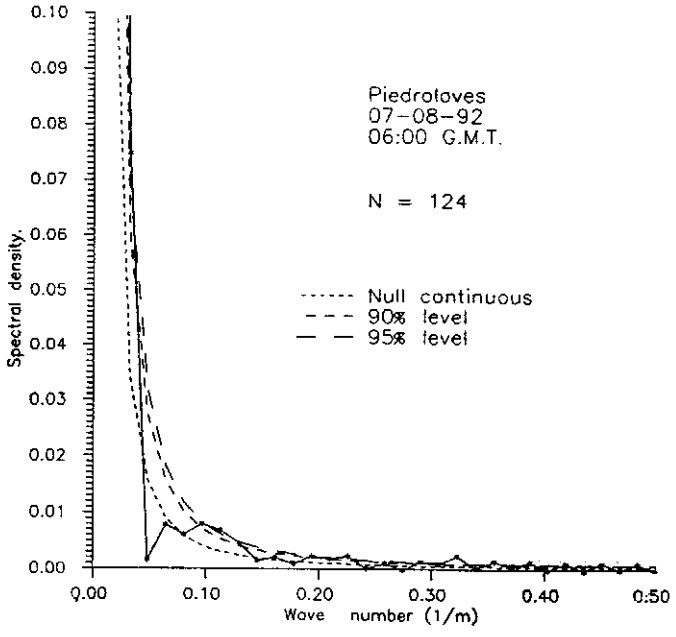

Figure 8. Power spectre. Piedralaves, 08/07/92. 06:00 G.M.T.

In Figure 8, which shows the power spectrum of the data registered on 6:00 July 8 at Piedralaves, we find two periodicities at the 95% level corresponding to wavelengths of 465 and 88 m.

Figure 9, which corresponds to a simultaneous sounding at Burgohondo, shows no periodicity at this level of confidence. At 08:00 we also find some periodicities at the downwind slope and none at the upwind one. At 12:00 we find no periodicity at either slope, which agrees with the instability of the atmosphere.

To find whether these periodicities are due to the observation place or to its relative position with respect to the incident flow, we analyse the spectra of Burgohondo registered on September 10, when this town was at the downwind slope.

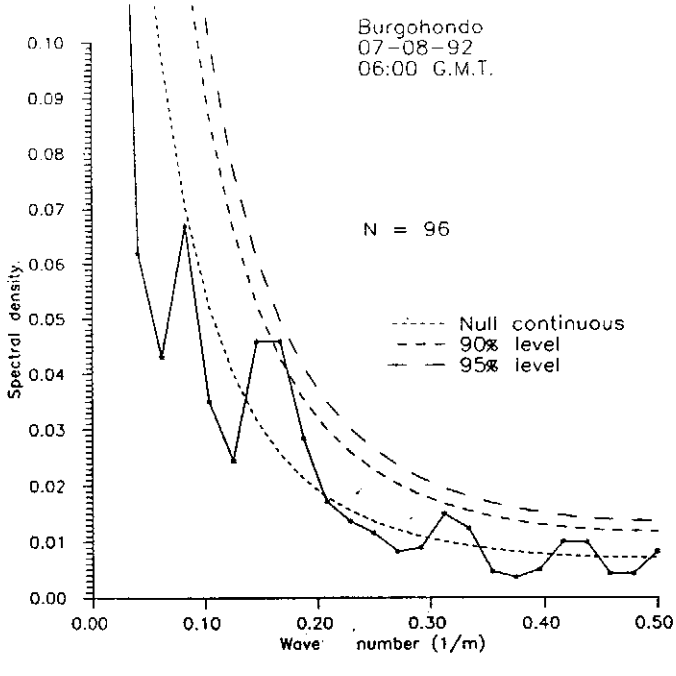

Figure 9. Power spectre. Burgohondo, 07/08/92. 06:00 G.M.T.

At 6:00 we find (Fig.10) two wavelengths of 23 and 130 m (Burgohondo) and none at Piedralaves (Fig.11). The rest of the results are like those of July 8. This way, we prove that the ondulatory patterns found are due to the relative position of the sites and not to their local topography.

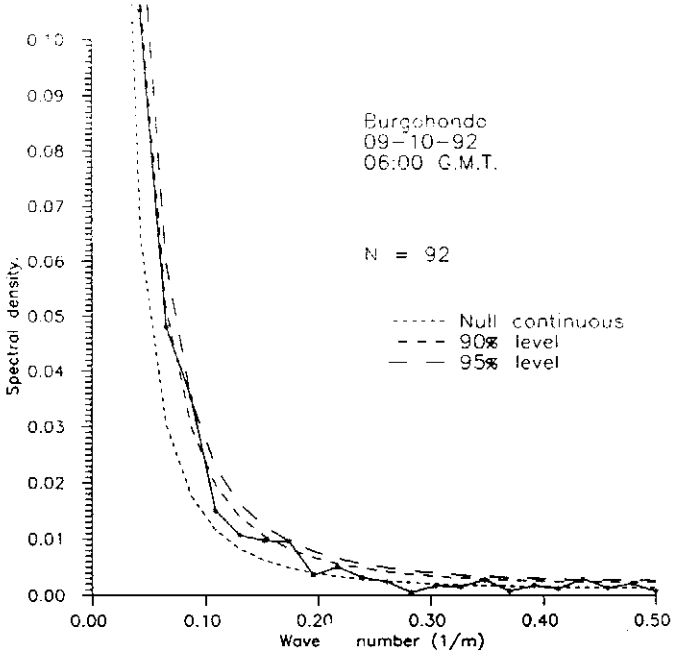

Figure 10. Power spectre. Burgohondo, 09/10/92. 06:00 G.M.T

7 Detection of lee vortices.

The spectral analysis doesn't help to identify the ondulatory patterns found in the numerical simulations by other authors. Scorer's parameter has the physical meaning of a wave number under stability of stratification. This is

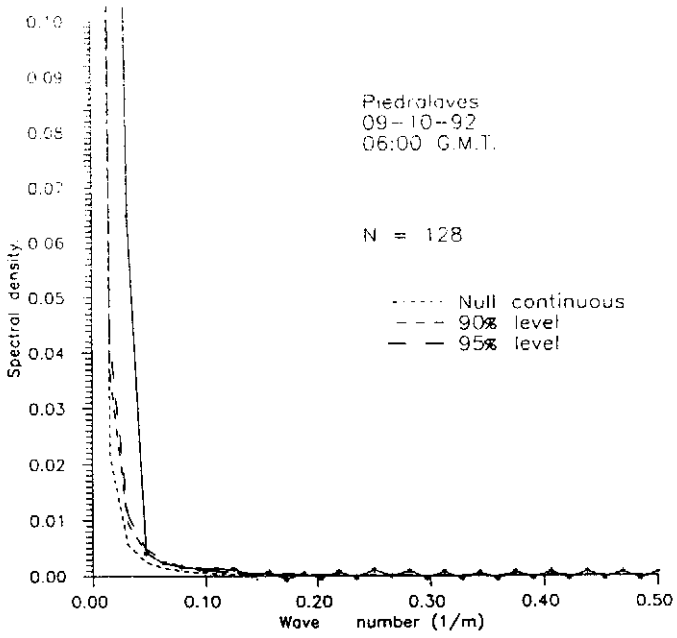

Figure 11. Power spectre. Piedralaves, 09/10/92. 06:00 G.M.T

the case for July 8 and September 10. If we choose a layer 200m thick, the associated wavelengths on July 8 are shown in Tab.15 and Tab.16. The dashed squares show unstable stratification and the empty ones, lack of data.

A first analysis of these tables shows that the shortest wavelengths are closest to the ground and appear in the early morning, under the greatest stability.

Hour	0-200m	200-400m	400-600m	600-800m	800-1000m
06:00	400	1800	4300	2000	600
08:00	----	1850	3900	1800	850
10:00	----	1900	2600	3800	800
12:00	----	----	2350	----	
16:00	----	3900	2400	6800	

Table 15. Wavelengths (m) associated to Scorer's parameter. Piedralaves, 07/08/92.

The wavelength increases as stability decreases. Table 2 (Fr values) will be used to analyse its evolution in time. Smolarkiewicz and Rotunno and Miranda and James found that if Fr is about 0.06 there is a vortex close to the ground and near the slope of the mountain. As Fr grows, the vortex goes up along the slope and reaches the top of the mountain for Fr about 0.22. For higher values of Fr these vortices disappear and the only ondulatory patterns found at the downwind slope are unbroken waves whose influence on this slope decreases as the perturbation propagates to upper layers.

Hour	0-200m	200-400m	400-600m	600-800m	800-1000m
06:00	350	650	800	1150	600
08:00	----	1150	1700	1200	
10:00	1150	4300	----	2250	2650
12:00	----	1350	----	2350	3750
16:00	----	3900	----	2650	

Table 16. Wavelengths (m) associated to Scorer's parameter. Burgohondo, 07/08/92.

The values in Table 2 are theoretically adequate to detect lee vortices in the early morning. Table 15 and Fig.12 indicate a vortex at some 600 m above Piedralaves, 200 m thick and 4300 m long at its widest point (Fig.13). Figures 14 and 15 show the evolution of the vortex at 8:00 and 10:00. In a similar way we found lee vortices over Burgohondo on September 10.

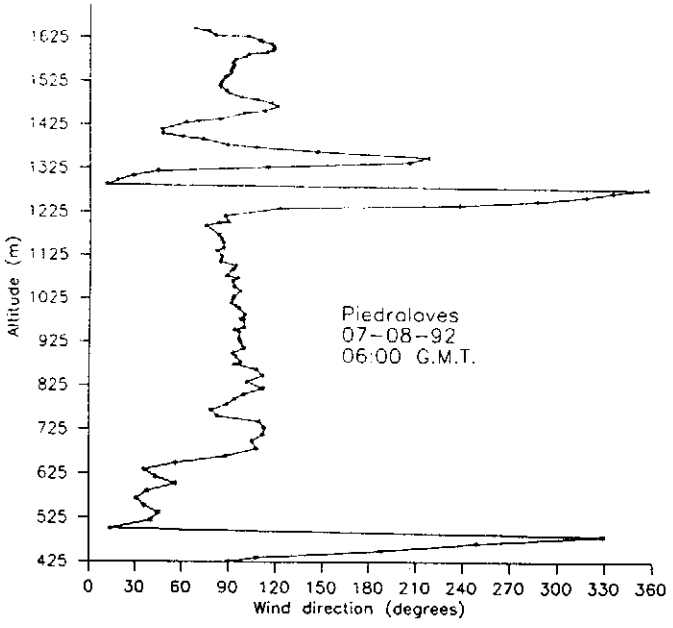

Figure 12. Wind direction-height. Piedralaves 07/08/92

06:00 G.M.T.

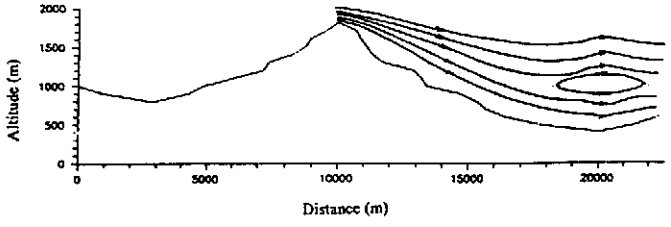

Figure 13. Lee vortices 07/08/92. 06:00 G.M.T.

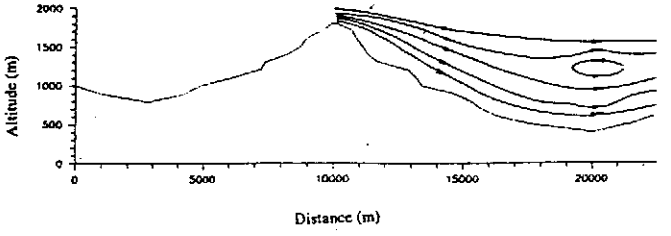

Figure 14. Lee vortices 07/08/92. 08:00 G.M.T.

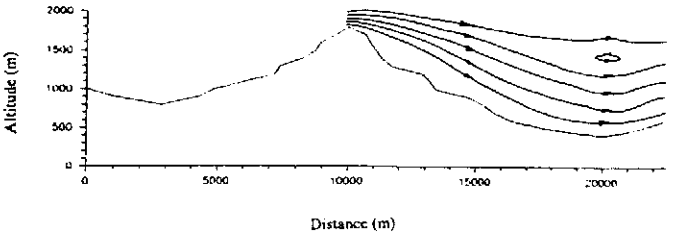

Figure 15. Lee vortices 07/08/92. 10:00 G.M.T.

8. Summary and conclusions.

In this work, we have analysed the behaviour of the atmosphere near an orographic obstacle according to the PBL data registered at both sides of a mountain range.

Following Holmboe and Klieforth (1957), and after an analysis of scale of the data registered, we have written Scorer's parameter without the terms of wind shear.

We have found out the conditions to extrapolate data from one slope to the opposite. Stagnation points at the downwind slope of a mountain range have been studied and proved their agreement with the theoretical predictions by Peltier and Clark (1979) and Smith (1988, 1989, 1993).

The existence of stagnation points above the slopes of the mountains partially corroborate Smith's nonlinear theory predictions (1993). The placement of downwind stagnation point (A) agrees with the predictions of nonlinear theory, but the upwind stagnation point (B) hasn't disappeared as its theory predicts.

The spectral analysis of the data showed the existence of ondulatory patterns at the downwind slope, which proved

their independence from local orography and their dependence on the relative position of the observation sites with respect to the flow.

Finally, we have drawn the lee vortices according to Scorer's wavelengths under stability of stratification and to detected changes in wind direction. Fr values are used to study their evolution in time, which agrees with Hunt and Snyder (1980), Smolarkiewicz and Rotunno (1989a) and Miranda and James (1992).

References.

Blanchard, D. O. and Howard, K. W. The Denver hailstorm of 13 June 1984. *Bull. Amer. Meteor. Soc., 67*, 1123-1131, 1986.

Brighton, P.W.M.. Strongly stratified flow past three- dimensional obstacles. *Quart. J. R. Met. Soc. 104*, 289- 307, 1978.

Castro, I. P. A note on lee wave structures in stratified flow over three-dimensional obstacles. *Tellus, 39A*, 72-81, 1987.

Crook, N. A., Clark, T. L. and Moncrieff, M. W.. The Denver Cyclone. Part I: Generation in low froude number flow. *J. Atmos. Sci. 47*, 2725-2742, 1990.

Díaz J. Variación espacial y temporal de los parámetros de estabilidad en orografía compleja y ondas de montaña. *Tesis Doctoral. U.C.M.*, 1993.

Drazin, P.G. On the steady flow of a fluid of variable density past an obstacle. *Tellus, 13*, 239-251, 1961.

Ferber, G. K. y Mass, C. F. Surface Pressure perturbations produced by an isolated mesoscale topographic barrier. Part I: General Characteristics and Dynamics. *Mon. Wea. Rev., 118*, 2579-2596, 1990 a.

Ferber, G. K. y Mass, C. F. Surface Pressure perturbations produced by an isolated mesoscale topographic barrier. Part II: Influence on regional Circulations. *Mon. Wea. Rev., 118*, 2597-2612, 1990 b.

Fosberg, M.A.. A diagnostic three-dimensional mass and momentum conserving wind model for complex terrain. Third Conference on Mountain Meteorology. 16-19 Oct. 1984. *Am. Meteor. Soc. Boston*, 13-16, 1984.

Hernández, E., Valero, F., Cano, J. L., Del Teso, M.T., Díaz J., García, A. A preliminary study for the development of a meteorological wind model in the area of Sierra de Gredos. *OMM. Proceedings Conference Météorologie et incendies des fôrets*. Rabat, Marruecos, 25-30 nov. 1991. Geneve, 1992 a.

Hernández, E., Díaz J., García A.. Modelo de diagnóstico del campo de viento en orografía compleja. *A.M.E. Encuentro Meteo 92, 1*, 109-116, 1992 b.

Hernández, E., Díaz J., García A. Modelo de diagnóstico para la dirección y velocidad del viento. *Rev. Geof. 48*, No. 2, 1993.

Holmboe, J. y Klieforth, H. Investigations of mountain lee waves and the air flow over the Sierra Nevada. *Dept. Met. Univ. California*, 1957.

Hunt, J. C. R. y Snyder, W. H.. Experiments on stably and neutrally stratified flow over a model three-dimensional hill. *J. Fluid Mech., 96*, 671-704, 1980.

Kelvin, L.. On stationary waves in flowing water. *Philos. Mag., 5*, 22, 353-357, 445-452, 517-530, 1886.

Miranda, P.M. A. y ames, I. N. Non-linear three-dimensional effects on gravity-wave drag: Splitting flow and breaking waves. *Q. J. Roy. Met. Soc. 118*, 1057-1081, 1992.

Peltier, W. R. y Clark, T. L.. The evolution and stability of finite-amplitude mountain waves: Part II. Surface wave drag and severe downslope windstorms. *J. Atmos. Sci., 36*, 1498-1529, 1979.

Queney, P.. Theory of perturbations in stratified currents with application to airflow over mountain barriers. *The University of Chicago Press, Misc. Rep., No. 23.*, 1947.

Rayleigh, R. J. The form of standing waves on the surface of running water. *Proc. London Math. Soc., 15*, 69-78, 1883.

Rottman, J. W. y Smith, R. B.. A laboratory model of severe downslope winds. *Tellus, 41A*, 401-415, 1989.

Scorer, R. S. Theory of waves in the lee of mountains. *Quart. J. R. Met. Soc., 75*, 41-56, 1949.

Sheppard, P.A.. Airflow over mountains. *Quart. J. R. Met. Soc. 82*, 159-161, 1956.

Smith, R. B., Linear theory of stratified hydrostatic flow past an isolated mountain. *Tellus, 32*, 348-364, 1980.

Smith, R. B. Linear theory of stratified flow past an isolated mountain in isosteric coordinates. *J. Atmos. Sci.,45*, 1988.

Smith, R. B.,. Mountain-induced stagnation points in hydrostatic flow. *Tellus, 41 A*, 270-274, 1989 a.

Smith, R. B.,. Comments on "Low Froude number flow past three-dimensional obstacles. Part I: Baroclinically generated lee vortices". *J. Atmos. Sci., 46*, 3611-3613, 1989 b.

Smith, R. B., Stagnation points and bifurcation in 3-D mountain flow. *Tellus, 45 A*, 28-43, 1993.

Smolarkiewicz, P. R., Rasmussen, R. M. y Clark, T. L. On the dynamics of Hawaiian cloud bands: island forcing. *J. Atmos. Sci. 45*, 1872-1905, 1988.

Smolarkiewicz, P. R. y Rotunno, R. Low Froude number flow past three-dimensional obstacles. Part I: Baroclinic generated lee vorticities. *J. Atmos. Sci. 46*, 1154-1164, 1989.

Smolarkiewicz, P. R. y Rotunno, R. Low Froude number flow past three-dimensional obstacles. Part II: Baroclinic generated lee vorticities. *J. Atmos. Sci. 47*, 1990.